Indications of nonlinear structures in brain electrical activity

Temujin Gautama,* Danilo P. Mandic,† and Marc M. Van Hulle‡

Laboratorium voor Neuro- en Psychofysiologie, K.U. Leuven, Campus Gasthuisberg, Herestraat 49, B-3000 Leuven, Belgium

The dynamical properties of electroencephalogram (EEG) segments have recently been analyzed by Andrzejak and co-workers for different recording regions and for different brain states, using the nonlinear prediction error and an estimate of the correlation dimension. In this paper, we further investigate the nonlinear properties of the EEG signals using two established nonlinear analysis methods, and introduce a "delay vector variance" (DVV) method for better characterizing a time series. The proposed DVV method is shown to enable a comprehensive characterization of the time series, allowing for a much improved classification of signal modes. This way, the analysis of Andrzejak and co-workers can be extended toward classification of different brain states. The obtained results comply with those described by Andrzejak *et al.*, and provide complementary indications of nonlinearity in the signals.

I. INTRODUCTION

In many applications of signal analysis, it is useful to verify the existence of an underlying nonlinear process, so that appropriate modeling or filtering techniques can be selected. In the field of biomedical signal processing, e.g., the analysis of heart rate variability, electrocardiogram, hand tremor, and electroencephalogram, the presence or absence of nonlinearity often conveys information concerning the health condition of a subject (for an overview, see Ref. [1]).

In particular, the electroencephalogram (EEG) signals are often examined using nonlinearity analysis techniques, as such, or by comparing signals that are recorded during different physiological brain states (e.g., during an epileptic seizure). The problem, however, as stated in Ref. [2], is that different analysis results can be either due to a genuine difference in dynamical properties of the brain, or due to differences in recording parameters. Recently, Andrzejak *et al.* have analyzed five sets comprising 100 EEG segments each, recorded extracranially in healthy subjects with eyes open and closed, and intracranially in epilepsy patients both during seizure-free intervals and epileptic seizures [2]. They have found the strongest indication of nonlinear deterministic dynamics for seizure activity, and no significant indication of nonlinearity for healthy subjects with eyes closed, by examining the predictability and the correlation dimension of the time series. Many methods exist for characterizing a time series, but, probably due to the strong interest in chaos, the applications have been typically concerned with detecting or analyzing nonlinear properties in a time series [3], but less with a characterization over different scales that remains invariant over multiple realizations of the underlying system.

To this cause, we propose a characterization method, the

"delay vector variance" (DVV) method, which we first use for performing a nonlinearity analysis, the aim of which is to verify whether or not a time series is generated by a linear stochastic system. The proposed method yields a standardized characterization of a time series that examines the local predictability over different scales. The method is applied to the five sets of EEG segments [2], and the obtained results are confirmed by those of two other, established methods. Due to the nature of the proposed method, the DVV method yields a reliable characterization of the EEG signals, which allows for an extension of the analysis described in Ref. [2] toward an accurate classification of different brain states.

II. METHODS

After a brief summary of the EEG data, we describe the basis of the statistical framework of the analysis (surrogate data). Next, two established nonlinearity analysis methods, the third-order autocorrelation function, and the asymmetry due to time reversal, are briefly addressed, and the proposed method is introduced.

A. Data

We have used the data described in Ref. [2], which is publicly available [13]. Therefore, we restrict ourselves to only a short description and refer to Ref. [2] for further details.

The complete dataset consists of five sets (denoted $A–E$), each containing 100 single-channel EEG segments of 23.6 s. Each segment has been selected after visual inspection for artifacts and has passed a weak stationarity criterion. Sets A and B have been taken from surface EEG recordings of five healthy volunteers with eyes open and closed, respectively. Segments in two sets have been measured in seizure-free intervals from five patients in the epileptogenic zone (D) and from the hippocampal formation of the opposite hemisphere of the brain (C). Set E contains seizure activity, selected from all recording sites exhibiting ictal activity. Sets A and B have been recorded extracranially, whereas sets C, D, and E have been recorded intracranially. Apart from the different

---

*Electronic address: temu@neuro.kuleuven.ac.be

†Present address: Department of Electrical and Electronic Engineering, Imperial College of Science, Technology and Medicine, Exhibition Road, SW7 2BT, London, U.K. Electronic address: d.mandic@ic.ac.uk

‡Electronic address: marc@neuro.kuleuven.ac.be

recording electrodes, the recording parameters were fixed. For this reason, different analysis results can be attributed to different dynamical properties of the brain.

B. Surrogate time series

Similar to the approach employed by Andrzejak *et al.* [2], the surrogate data method is used for assessing the nonlinearity present in the time series. A surrogate time series, or "surrogate" for short, is a realization of a "composite" null hypothesis, in our case that the original time series is generated by a Gaussian linear and stationary process, measured by a memoryless, monotonic and possibly nonlinear observation function (for an overview, see Ref. [3]). As suggested by Theiler and Prichard [4], metrics can be used for characterizing the original signal which can be compared to those obtained for an ensemble of surrogate time series using a nonparametric rank-based test. The hypothesis tests in this paper are performed at the level of $\alpha=0.02$. For a set of EEG segments, the number of time series in a set for which the null hypothesis is rejected is referred to as the "rejection rate."

For every original time series, the surrogates are generated using the iterative amplitude adjusted Fourier transform (iAAFT) method described by Schreiber and Schmitz [3]. The iAAFT generated surrogates have their amplitude spectra similar, and their amplitude distributions identical to that of the original time series. Using a significance level of $\alpha=0.02$, the null hypothesis for a right-tailed test with 49 surrogates is rejected if the rank of the original test statistic is equal to 50, and for a two-tailed test with 99 surrogates if the rank is equal to 1 or equal to 100.

C. Nonlinearity measures

In the following analysis, the delay vector variance method is compared to two other, established measures of nonlinearity, which have also been used in Ref. [5], namely, the third-order autocovariance (C3) and the asymmetry due to time reversal (REV). The third-order autocovariance is a higher-order extension of the traditional autocovariance and is given by

$$t^{C3}(\tau)=\langle x_k x_{k-\tau} x_{k-2\tau}\rangle, \qquad (1)$$

where τ is a time lag. A time series is said to be reversible if its probabilistic properties are invariant with respect to time reversal. A possible measure for the asymmetry due to time reversal is

$$t^{REV}(\tau)=\langle (x_k-x_{k-\tau})^3\rangle. \qquad (2)$$

It has been shown in Ref. [5] that, in combination with the surrogate data method, these two measures yield reliable two-tailed tests for nonlinearity. For convenient comparison to the results described in Ref. [2], the time lag τ is set to unity [14] in all simulations for both test statistics.

D. Proposed method: Delay vector variance method

Although established methods in the field of nonlinearity analysis exist, such as the two methods described in the pre-

ceding section, there is a need for a robust method which is straightforward to interpret and visualize. To be able to perform reasonably well on a wide variety of signals, it is desirable that such a method makes use of some well-established notions from nonlinear dynamics and chaos, such as the embedding dimension and geometry in phase space. The existing methods are often complex and specific, e.g., the deterministic versus stochastic (DVS) plots [6], and the correlation dimension [7,8].

Therefore, we propose an analysis of a time series which examines the predictability of a time series in phase space at different scales, using the method of time delay embedding for representing a time series: for a given embedding dimension m, a set of delay vectors (DVs), $\mathbf{x}(k)=[x_{k-m\tau},\ldots,x_{k-\tau}]$, is generated, where τ is a time lag which for convenience is set to unity in all simulations. This choice of τ is a conservative one in the context of nonlinearity detection. Indeed, assuming the embedding dimension is sufficiently high (as can be expected in our case, since it was determined using Cao's method), a linear time series can be accurately represented using $\tau=1$, whereas this is not the case for a nonlinear signal, for which the time lag plays an important role in its characterization. Therefore, if the null hypothesis of linearity is rejected, one can safely assume that the time series is nonlinear (since the linear part was accurately described for $\tau=1$, and the rejection can be attributed to the nonlinear part of the signal). Conversely, if the null hypothesis is found to hold, this can be due to the fact that either the signal is genuinely linear, or that the signal is nonlinear and that the phase space was poorly reconstructed using $\tau=1$.

Every DV $\mathbf{x}(k)$ has a corresponding *target*, namely, the next sample, x_k. The proposed approach is somewhat related to the δ-ϵ method [9] and the deterministic versus stochastic plots [6], both of which are local prediction techniques, and the correlation sum [7] which characterizes reconstructed attractors over different distance scales in phase space. The latter has also been used for comparing time delay embedded time series [10].

For a given embedding dimension m, the proposed method computes the mean target variance σ^{*2} over all sets Ω_k. A set Ω_k is generated by grouping those DVs that are within a certain distance to $\mathbf{x}(k)$, which is varied in a manner standardized with respect to the distribution of pairwise distances between DVs. This way, the threshold scales automatically with the embedding dimension m, as well as with the dynamical range of the time series at hand, and thus, the complete range of pairwise distances is examined. The proposed delay vector variance method can be summarized as follows.

(a) For a given embedding dimension m: The mean μ_d and standard deviation σ_d are computed over all pairwise Euclidean distances between DVs, $\|\mathbf{x}(i)-\mathbf{x}(j)\|$ $(i\neq j)$.

(b) For a given embedding dimension m: The sets $\Omega_k(r_d)$ are generated such that $\Omega_k(r_d)=\{\mathbf{x}(i)|\ \|\mathbf{x}(k)-\mathbf{x}(i)\|\leqslant r_d\}$, i.e., sets which consist of all DVs that lie closer to $\mathbf{x}(k)$ than a certain distance r_d, taken from the interval $[\max\{0,\mu_d-n_d\sigma_d\};\mu_d+n_d\sigma_d]$, e.g., uniformly spaced, where n_d is a

parameter controlling the span over which to perform the DVV analysis.

(c) For a given embedding dimension m: For every set $\Omega_k(r_d)$, the variance of the corresponding targets, $\sigma_k^2(r_d)$, is computed. The average over all sets $\Omega_k(r_d)$, normalized by the variance of the time series, σ_x^2, yields the measure of unpredictability $\sigma^{*2}(r_d)$,

$$\sigma^{*2}(r_d) = \frac{\frac{1}{N}\sum_{k=1}^{N} \sigma_k^2(r_d)}{\sigma_x^2}. \qquad (3)$$

We only consider a variance measurement to be *valid*, if the set $\Omega_k(r_d)$ contains at least 30 DVs.

As a result of the standardization of the distance axis, the resulting DVV plots are straightforward to interpret. The presence of a strong deterministic component will lead to small target variances for small spans. At the extreme right, the DVV plots smoothly converge to unity, since for maximum spans, all DVs belong to the same set, and the variance of the targets is equal to the variance of the time series. If this is not the case, the span parameter n_d should be increased. Thus, visual inspection of the convergence of a DVV plot to unity at the extreme right should be used for setting this parameter (we typically start from $n_d = 2$ and increase it using unit steps until the DVV plots converge to unity at the extreme right). Note that the DVV plot yields a characterization of the time series at different scales and goes beyond an estimate of the deterministic or stochastic component. In all simulations, the parameter n_d was set to four, and the interval $[\mu_d - n_d\sigma_d; \mu_d + n_d\sigma_d]$ was divided into 100 equidistant r_d values.

In the following step, the linear or nonlinear nature of the time series is examined by performing DVV analyses with identical parameters for both the original and a number of surrogate time series. Due to the standardization of the distance axis, these plots can be conveniently compared using the test statistic t^{DVV}, namely, the root mean square error (RMSE) between the σ^{*2}'s of the original time series and the σ^{*2}'s averaged over the DVV plots of the surrogate time series (note that when computing this average, as well as when computing the RMSE, only the valid measurements are taken into account):

$$t^{\text{DVV}} = \sqrt{\left\langle \left(\sigma^{*2}(r_d) - \frac{\sum_{i=1}^{N_s} \sigma_{s,i}^{*2}(r_d)}{N_s} \right)^2 \right\rangle_{\text{valid } r_d}}, \qquad (4)$$

where $\sigma_{s,i}^{*2}(r_d)$ is the target variance at span r_d for the ith surrogate, and the average is taken over all spans r_d that are valid in all surrogate and original DVV plots. In this way, a single test statistic is obtained, and traditional (right-tailed) surrogate testing can be performed (the RMSE to the average is computed for the original, and surrogate time series).

TABLE I. Number of time series for which the null hypothesis of linearity is rejected (rejection rate) at the level of $\alpha = 0.02$ for the different sets. For comparison, the rejection rates described in Ref. [2], obtained at the level of $\alpha = 0.025$ are also included (denoted by P and $D_{2,eff}$, see discussion section). The last column gives the rejection rates using the minimal target variance ($\sigma_{\min}^{*2}$, see Sec. IV).

Set	C3	REV	DVV	P	$D_{2,eff}$	$\sigma_{\min}^{*2}$
A	8	15	29	4	0	4
B	8	37	32	9	0	8
C	20	23	46	14	7	5
D	20	41	53	37	27	18
E	65	86	92	89	27	70

III. RESULTS

In the simulations, we aim at extending the nonlinearity detection results described in Ref. [2] to a classification of the EEG segments. To that cause, first the results for the individual nonlinearity analyses are presented. Subsequently, the test statistics for the three methods (C3, REV, and DVV) are used for classification purposes.

A. Nonlinearity analysis

To compare our methodology to that adopted by Andrzejak and co-workers [2], we have performed nonlinearity analyses on each of the 500 EEG segments. For several time series in the five sets, the minimum embedding dimensions have been determined using Cao's method [11], yielding $m = 10$. In all DVV analyses, the embedding dimension is set to $m = 10$ and $n_d = 4$. The rejection rate, that is, the number of time series for which the composite null hypothesis of linearity has been rejected, is shown in Table I. It can be clearly seen that set E has a higher rejection rate than the other sets. Note that the probability of having n_{rej} or less time series rejected at the level of $\alpha = 0.02$ by pure chance in a set of 100 time series, is 1.89×10^{-4} for $n_{\text{rej}} = 8$ [2]. Thus, all sets $A - E$ show significant indications of nonlinearity for all methods (C3, REV, and DVV).

Figure 1 shows the average DVV plots for the different sets. It can be clearly seen that sets A and B, and C and D
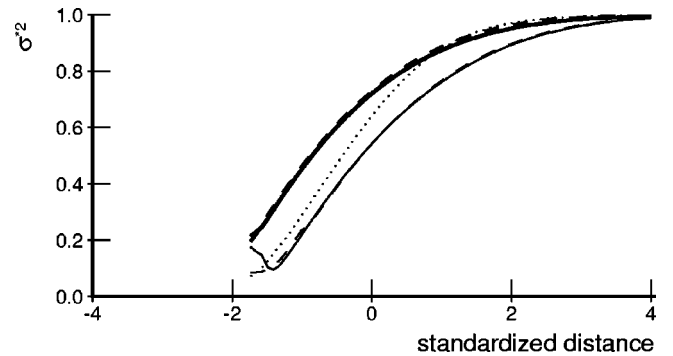

FIG. 1. Average DVV plots for the five sets of time series: A (thick solid), B (thick dashed), C (thin solid), D (thin dashed), and E (dotted).

TABLE II. The classification performances for the different methods and setups, expressed as a percentage.

Method	NNC5	LOOC5	NNC3	LOOC3
C3	20.6	26.2	31.6	42.2
REV	30.2	35.4	42.2	51.8
DVV	47.2	60.8	74.4	86.2

yield similar DVV plots. As already described in the methods section, by design, all DVV plots converge to unity at the right hand side of the standardized distance axis. The minimal target variance for the DVV plots, which is an indication of the predictability of the time series, is lower for sets C, D, and E (epilepsy patients), than for sets A and B (healthy subjects).

B. Classification

In this section, the applicability of the various methods are examined with respect to the characterization of the time series. We examine whether or not these methods allow for a classification of the time series into the different categories. Every time series has a desired label, namely, that of the set from which it is taken, and the objective of the classifier is to correctly label each of the 500 time series. We consider two cases: the five-class case and the simplified three-class case, which groups classes A and B, and classes C and D. Every time series is characterized by a feature vector on which the classification is performed. For the first two methods (REV and C3), this is simply the test statistic, but for the DVV method, the vector containing the target variances for certain standardized distances is used. We limit the feature vectors to those standardized distances for which all DVV analyses yield valid target variances.

Although there exist many methods for supervised classification (the desired labels are known *a priori*), we restrict our analysis to two methods, which can be interpreted as a lower and upper bound of possible classification systems.

Nearest neighbor classification (NNC). The class prototypes are determined as the average of the feature vectors of all time series belonging to a certain set. The class label of a time series is determined as that of the prototype which is nearest to its feature vector (L_2 norm).

Leave-one-out classification (LOOC). The label of a time series i is determined by leaving out this time series, and considering the remaining set of feature vectors as the set of labeled prototypes. The label of time series i is set equal to that of the nearest prototype.

The classification performances are expressed as the fraction of correct classifications, and are shown in Table II for the different setups, denoted by NNC5 and LOOC5 for the nearest neighbor and leave-one-out classification of the five-class case, and by NNC3 and LOOC3 for the respective three-class case. The classification performances for the DVV method (third row) outperform those for REV (first row) and C3 (second row) for all setups.

IV. DISCUSSION

We have introduced a methodology for characterizing the nature of a time series. The DVV method takes into account different properties of a time series, namely, time delay embedding, phase space geometry, and predictability. Furthermore, it has been shown that the feature vector extracted from the DVV analysis, using identical parameters for all time series, enables a comprehensive characterization of the dynamical modes of the EEG signals, allowing for an accurate classification of the brain states. The proposed method has been applied to the problem addressed in Ref. [2], which is a subject of much on-going research.

Andrzejak *et al.* [2] examined the nonlinear prediction error P in the phase space (embedding dimension $m=6$), at a prediction horizon of $H=65$ sampling times, and an estimate of the effective correlation dimension $D_{2,eff}$. They report an overall lower rejection rate than our findings (for comparison, the rejection rates obtained in Ref. [2] are included in Table I, labeled P and $D_{2,eff}$). This could be due to a restricted characterization of the time series, which is a very common issue in nonlinearity analysis. Indeed, nonlinearity and determinism are often confounded, as the presence of both is necessary for the existence of deterministic chaos (for a more detailed discussion, see Refs. [3,12]). Thus, when characterizing a time series on the basis of the nonlinear prediction error, only the deterministic structure is taken into account, which is not a property unique to nonlinear signals. Thus, the linear surrogates can have the same predictability as their nonlinear counterparts. Furthermore, as explained in Ref. [2], a difference in rejection rates can be attributed to either a higher sensitivity or a lower specificity of a method.

For comparison, we have examined the time series in the five EEG sets with respect to their deterministic structure, using the lowest target variance in the DVV plot, σ^{*2}_{min}, which corresponds to the mean square error (MSE) for the best performing local linear model, for an embedding dimension of $m=10$. As is the case for P, the rejection rates are considerably lower than those for REV, C3, and DVV, as shown in Table I (last column).

On the set level, Andrzejak *et al.* tentatively ranked the time series in decreasing order of the values of P, averaged over each of the five EEG sets, resulting in $A>C>B>D>E$. Similarly, we rank the DVV test statistics obtained for the DVV in increasing order and obtain: $B(0.0114)<A(0.0115)<C(0.0123)<D(0.0178)<E(0.0450)$. It can be observed clearly that in both analyses, the EEG activity during seizure-free intervals in the epileptogenic zone (D), and the EEG activity during a seizure (E) show more evidence for an underlying nonlinear process (DVV) and determinism (nonlinear prediction error, see Ref. [2]) than the other sets.

As shown by the classification results, the proposed DVV method provides a sufficiently detailed characterization of the EEG time series to distinguish between the different classes (surface recordings of healthy volunteers, intracranial EEG recordings of epilepsy patients from the seizure-free intervals, and from epileptic seizure activity). The performance of a classifier is expected to lie between 74.4% and

86.2%, as shown by our analyses. However, performance degrades for a more detailed classification which further dissociates between sets *A* (healthy volunteer, eyes open) and *B* (healthy volunteer, eyes closed), and sets *D* (epileptogenic zone) and *C* (hippocampal formation of opposite hemisphere). Therefore, we conclude that the proposed DVV characterization although not requiring any prior knowledge about a signal in hand is very robust, and exhibits improved performance over other available methods for a relatively crude clustering of multimodal signals into the basic classes. For a classification within the established classes, however, the DVV characterization as such is not detailed enough, and should be combined with additional measures, which are not based upon the geometry and predictability in phase space.

Overall, our results agree well with those obtained by Andrzejak *et al.* [2], with the exception that they found no (significant) indications of nonlinearity in the EEG segments recorded extracranially during the relaxed state of healthy subjects with eyes closed. The proposed DVV method clearly distinguishes between EEG segments recorded in healthy subjects, in epilepsy patients during a seizure-free interval, and during an epileptic seizure, indicating different dynamical properties of brain electrical activity.

[1] T. Schreiber, Phys. Rep. **308**, 2 (1999).

[2] R. Andrzejak, K. Lehnertz, F. Mormann, C. Rieke, P. David, and C. Elger, Phys. Rev. E **64**, 061907 (2001).

[3] T. Schreiber and A. Schmitz, Physica D **142**, 346 (2000).

[4] J. Theiler and D. Prichard, Physica D **94**, 221 (1996).

[5] T. Schreiber and A. Schmitz, Phys. Rev. E **55**, 5443 (1997).

[6] M. Casdagli, J. R. Stat. Soc. Ser. B. Methodol. **54**, 303 (1991).

[7] P. Grassberger and I. Procaccia, Physica D **9**, 189 (1983).

[8] R. Hegger, H. Kantz, and T. Schreiber, Chaos **9**, 413 (1999).

[9] D. Kaplan, Physica D **73**, 38 (1994).

[10] A. Albano, P. Rapp, and A. Passamante, Phys. Rev. E **52**, 196 (1995).

[11] L. Cao, Physica D **110**, 43 (1997).

[12] J. Theiler, S. Eubank, A. Longtin, B. Galdrikian, and J. Farmer, Physica D **58**, 77 (1992).

[13] URL: http://www.meb.uni-bonn.de/epileptologie/science/physik/eegdata.html

[14] The role of the time lag τ is discussed in the following section.